

# Journal of Biomedical Optics

[SPIEDigitalLibrary.org/jbo](http://SPIEDigitalLibrary.org/jbo)

## **Dual/differential coherent anti-Stokes Raman scattering module for multiphoton microscopes with a femtosecond Ti:sapphire oscillator**

Bei Li  
Paola Borri  
Wolfgang Langbein

# Dual/differential coherent anti-Stokes Raman scattering module for multiphoton microscopes with a femtosecond Ti:sapphire oscillator

Bei Li,<sup>a</sup> Paola Borri,<sup>b</sup> and Wolfgang Langbein<sup>a</sup>

<sup>a</sup>Cardiff University, School of Physics and Astronomy, Cardiff CF24 3AA, United Kingdom

<sup>b</sup>Cardiff University, School of Biosciences, Cardiff CF10 3US, United Kingdom

**Abstract.** In the last decade, coherent anti-Stokes Raman scattering (CARS) microscopy has emerged as a powerful multiphoton imaging technique offering label-free chemical sensitivity and high three-dimensional resolution. However, its widespread application in the life sciences has been hampered by the use of costly pulsed lasers, the existence of a nonresonant background requiring involved technical solutions for its efficient suppression, and the limited acquisition speed of multiplex techniques addressing several vibrational resonances, if improved chemical specificity is needed. We have recently reported a differential CARS technique (D-CARS), which simultaneously measures two vibrational frequencies, enhancing the chemical selectivity and sensitivity without introducing costly hardware, while maintaining fast acquisition. In this study, we demonstrate a compact, fully automated, cost-effective module, which integrates on hardware and software level with a commercial multiphoton microscope based on a single 100 fs Ti:Sapphire oscillator and enables D-CARS microscopy in a user-friendly format for applications in the life sciences. © The Authors. Published by SPIE under a Creative Commons Attribution 3.0 Unported License. Distribution or reproduction of this work in whole or in part requires full attribution of the original publication, including its DOI. [DOI: 10.1117/1.JBO.18.6.066004]

Keywords: coherent anti-Stokes Raman scattering; differential coherent anti-Stokes Raman scattering; microscopy.

Paper 130078R received Feb. 10, 2013; revised manuscript received May 8, 2013; accepted for publication May 10, 2013; published online Jun. 3, 2013.

## 1 Introduction

Optical microscopy is an indispensable tool that has driven progress in the life sciences, and is still the only practical means of obtaining subcellular spatial resolution within living cells and tissues. In the last decade, coherent anti-Stokes Raman scattering (CARS) has emerged as a powerful technique for chemically specific label-free imaging of living cells.<sup>1</sup> CARS is a third-order nonlinearity where molecular vibrations in the focal volume are coherently driven by a modulated laser intensity, enhancing their Raman scattering by constructive interference. Intrinsic three-dimensional (3-D) optical sectioning is provided by the nonlinearity, and the use of near-infrared excitation wavelengths increases the penetration depth into scattering tissue similar to two-photon fluorescence (TPF). However, there are two roadblocks for the widespread use of CARS in the life-science community.

First, since Raman resonances of biomolecules typically have picosecond coherence times, their excitation is optimized using picosecond pulses. Since two synchronized pulses of different wavelengths (pump and Stokes) are needed to create the modulated intensity, which coherently drives molecular vibrations, a typical laser choice for CARS is a picosecond laser pumping an optical parametric oscillator.<sup>1</sup> On the other hand, commercial multiphoton microscopes use 100 fs Ti:Sapphire lasers for efficient second harmonic generation (SHG) and TPF, for which picosecond sources give an order of magnitude less signal. Second, the chemical specificity is limited if only a

single vibrational frequency is detected, however, simultaneous excitation and detection of several vibrational resonances in multiplex CARS results in long acquisition times usually incompatible with live cell imaging.<sup>2</sup> Moreover, CARS is limited by a nonresonant background.

It has been demonstrated recently that one can achieve a tunable spectral resolution of the CARS excitation process with femtosecond pulses by controlling the pulse chirp using glass dispersion<sup>3</sup> to yield a constant instantaneous frequency difference (IFD) of pump and Stokes, a method called “spectral focussing.”<sup>4</sup> Furthermore, a photonic crystal fiber (PCF) with two zero-dispersion points can be used to create a Stokes pulse with a smooth spectral phase from a 100 fs Ti:Sapphire laser,<sup>5</sup> which together with spectral focussing allows for CARS microscopy.<sup>6</sup> It was also shown recently by our group that spectral focussing allows for a simple passive method<sup>7</sup> which we called differential CARS (D-CARS) to probe two (or more<sup>8</sup>) vibrational frequencies simultaneously while retaining fast acquisition speeds, and effectively rejects the nonresonant background. In this paper, we combined the single-frequency CARS approach of Ref. 6 with our D-CARS method and developed a compact, fully automated module providing a user-friendly upgrade of commercial multiphoton microscopes. Specifically, the capability of this D-CARS module was demonstrated on a Zeiss LSM 510 Meta two-photon and confocal microscope, where it was added between the laser source and the beam scanning head and integrated both at hardware and software levels (see Video 1). The resulting fast and efficient acquisition of CARS and D-CARS in cells and tissues combined with automated switching to TPF, and SHG contrast provided powerful multimodal imaging.

Address all correspondence to: Bei Li, Cardiff University, School of Physics and Astronomy, Cardiff CF24 3AA, United Kingdom. Tel: +44 (0) 29 208 70611; Fax: +44 (0) 29 208 74056; E-mail: [spxbl@cf.ac.uk](mailto:spxbl@cf.ac.uk)

## 2 Optical Setup

The optical layout of the module is shown in Fig. 1. A mode-locked Ti:sapphire laser provides pulses of about 100 fs duration at a repetition rate of  $T_r^{-1} = 90$  MHz and a power of 1.7 W (Coherent Chameleon). For the results shown later, the laser spectrum was centered at 790 nm and had a FWHM of 9.8 nm. The intensity of the laser was controlled by the TeO<sub>2</sub> acousto-optic modulator (AOM) of the Zeiss LSM510 used in this work. To compensate for the group delay dispersion (GDD) of about 18,000 fs<sup>2</sup> introduced by the AOM and the other optical components up to the PCF, a prism compressor was introduced between the laser and the AOM. The laser can be routed directly to the microscope by the FM to enable its original functionality. For CARS, the FM is removed and the beam is expanded and collimated in BE1 to result in a Gaussian beam waist of  $w_0 = 1.5$  mm, and a Rayleigh range of  $z_0 = 2$  m providing an acceptable beam divergence over the optical path of the setup. The half-wave plate HWP1 (WPA1212-2) rotates the linear polarization direction, which initially is in the plane of the setup. The beam is split by PBS1 (Thorlabs PBS102), with an intensity ratio adjusted by HWP1. The reflected beam is used as pump  $\omega_p$ . The transmitted beam is directed by the piezoelectrically actuated mirror M1 and coupled in and out of the PCF (Newport FemtoWhite CARS) by oil immersion lenses (Nikon CFI Plan Achromat 50X). Using an immersion oil index-matched to fused silica (Cargille 06350) suppresses the surface reflection so that an optical isolator<sup>6</sup> can be omitted. The PCF has two zero dispersion wavelengths around 775 and 945 nm and creates a continuum at 580 to 730 nm and 950 to 1150 nm with a well-defined chirp and low-intensity noise. The power coupled into the fiber was approximately 300 mW. The infrared branch of the continuum is used as Stokes beam  $\omega_s$ . The visible branch of the continuum can be used as pulsed source for fluorescence lifetime imaging. For a pump of 790 nm wavelength, a vibrational wave number

from 2000 to 3500 cm<sup>-1</sup> can be accessed, which can be extended down to 1000 cm<sup>-1</sup> using higher pump wavelengths. The Stokes is transmitted through an absorptive filter  $F$  (3 mm of RG850 at the Brewster angle of 55 deg) to remove the light overlapping with the CARS spectral region. The intensity of the pump is adjusted by HWP2 and the polarizer P1, delayed by a retro-reflector R on a motorized linear stage, and recombined with the Stokes by a dichroic beam splitter (DBS) (CVI LWP-45-Rp-800-Tp-946-PW-1025-C). The pump pulse arrival time at  $t_0$  relative to the Stokes (negative for pump leading) is adjusted by the linear stage, allowing one to change the IFD by a delay-scan. To set equal linear chirp of pump and Stokes for spectral focusing with adjustable pulse duration,<sup>3</sup> glass blocks of known GVD (SF57) are inserted. The Stokes propagates through GB1 of thickness  $L_1$  adjustable between 0 and 110 mm with 10 mm steps, and after recombination in the DBS pump and Stokes propagate through GB2 of thickness  $L_2$  adjustable between 0 to 160 mm with 20 mm steps. Example spectra of the pump and Stokes beam are shown in Fig. 2 together with a nonresonant CARS spectrum generated for  $L_1 = 30$  mm and  $L_2 = 0$  mm by focusing the beam after GB3 through a high index ball lens and detected by a spectrometer integrated into the module.

For D-CARS,<sup>7</sup> a second polarizer P2 after the DBS projects pump and Stokes to horizontal linear polarization, after which the polarization direction is rotated by HWP3, adjusting the splitting ratio in the subsequent polarizing beam splitter PBS2 which creates two copies of the pulse pair  $\Pi_1$  and  $\Pi_2$ . The reflected  $\Pi_2$  is traveling over 1.7 m, resulting in a propagation time of half the laser repetition period  $T_r/2$ , before being spatially recombined with  $\Pi_1$  in the polarizing beam splitter PBS3.  $\Pi_2$  passes a third glass block GB3 of thickness  $L_3$  which is adjustable from 0 to 21 mm with 1 mm steps. Due to the lower group velocity of the pump compared to the Stokes in GB3, the IFD of  $\Pi_2$  is reduced by an amount  $\Delta_{\text{IFD}}$  which is approximately linear with  $L_3$ .

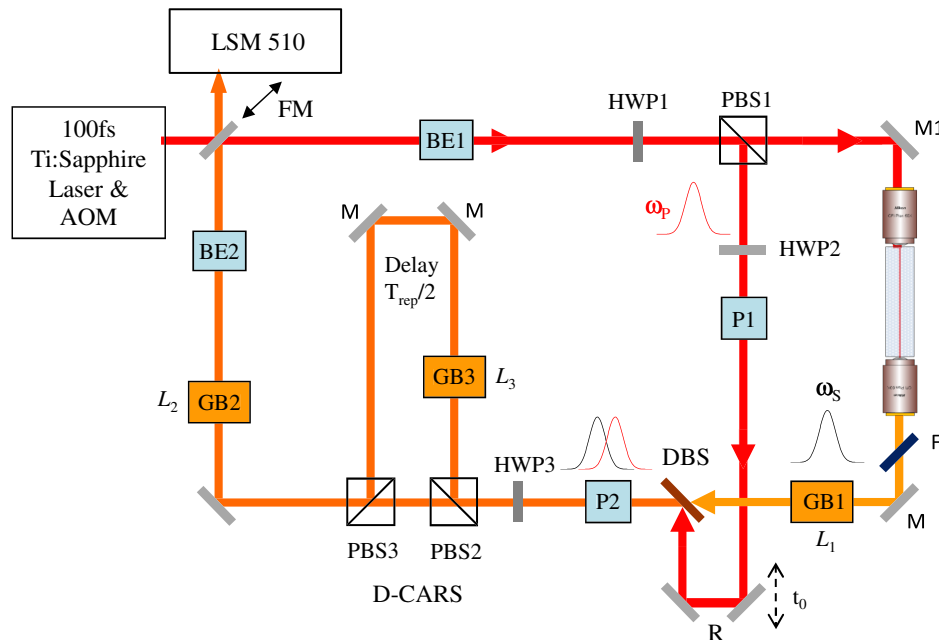


**Fig. 1** Sketch of the optical setup (Video 1).  $\omega_p$  and  $\omega_s$ : pump and Stokes beams, FM: flip mirror, BE: beam expander, PCF: photonic crystal fiber, M: sliver mirror, HWP: half-wave plate, P: polarizer, PBS: polarizing beam splitter, D: dichroic mirror, F: filter, R: retroreflector, GB: glass blocks, and LSM 510: Zeiss LSM 510 multiphoton microscope (MPEG, 3.1 MB) [URL: <http://dx.doi.org/10.1117/1.JBO.18.6.066004.1>].

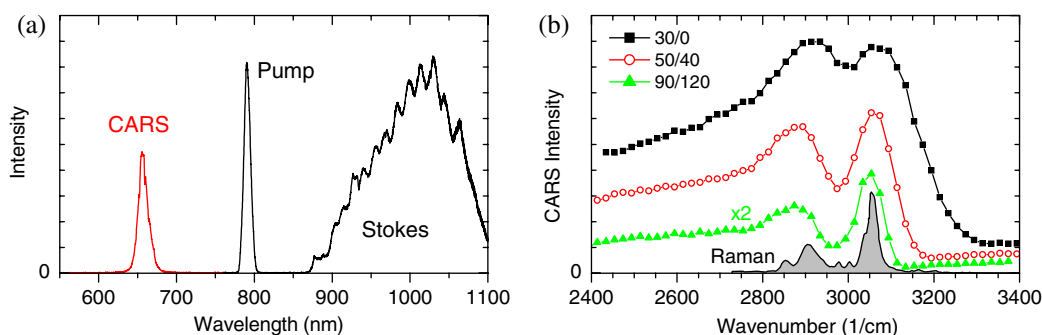


**Fig. 2** (a) Spectral intensity of pump, Stokes, and generated nonresonant coherent anti-Stokes Raman scattering (CARS) signal at an IFD of  $2585\text{ cm}^{-1}$ . (b) CARS spectra of polystyrene measured with different lengths of SF57  $L_{1,2}$  as labeled in mm. Relative scaling factors are given. Power at the sample pump is 36 mW and Stokes is 4 mW.

To measure the CARS intensity at the laser repetition rate needed for D-CARS<sup>7</sup> in conjunction with the dc component measured by the nondescanned detector (NDD) detector of the LSM510, we have modified the detector, routing the high-frequency component of the PMT anode current ( $>10\text{ MHz}$ ) through a 25 dB amplifier via a 50 Ohm coaxial cable to a home-built analog high-frequency lock-in amplifier. The low-frequency (LF) components ( $<10\text{ MHz}$ ) are transmitted to the NDD module. The lock-in amplifier is referenced to the laser repetition rate, and its phase is adjusted to the CARS signal  $I_{\text{CARS}}(\Pi_2)$  from  $\Pi_2$ . The lock-in output with a bandwidth of 1 MHz is fed into a dummy NDD detector unit of the LSM510 enabling its acquisition with by the LSM510 software. In this way, the difference  $I_{\text{dif}} = I_{\text{CARS}}(\Pi_2) - I_{\text{CARS}}(\Pi_1)$  and sum  $I_{\text{sum}} = I_{\text{CARS}}(\Pi_2) + I_{\text{CARS}}(\Pi_1)$  of the CARS of the two pairs are acquired simultaneously. In  $I_{\text{dif}}$  the nonresonant CARS background can be suppressed<sup>7</sup> by balancing the contributions of both pairs using HWP3, enhancing the chemical selectivity and sensitivity. Alternatively, two independent vibrational frequencies with up to  $500\text{ cm}^{-1}$  difference can be measured simultaneously.

The optical setup was implemented in a square module of 60-cm side length. The spatial mode overlap of pump–Stokes and  $\Pi_1 - \Pi_2$ , and the coupling into the PCF is adjusted by tip–tilt piezoelectric actuators on PBS1, PBS2, and PBS3. The HWPs are servo-actuated as well as beam shutters for pump, Stokes,  $\Pi_1$ , and  $\Pi_2$ . The module was attached to the Zeiss LSM 510 between the AOM and the scanner input. In this way, multimodal microscopy is enabled, including the multiphoton techniques SHG, TPF, CARS, and D-CARS as well as confocal fluorescence. The module was tested on different samples using a  $20 \times 0.8\text{ NA}$  plan-Apochromat objective (Zeiss 440640-9902-000). The power at the sample for pump and Stokes were typically 50 and 7 mW, respectively. The transmission from the input of the scan head to the sample for pump (Stokes) was 64% (22%), respectively.

### 3 Results and Discussion

The tuneable spectral resolution in CARS by spectral focusing obtained with the module is shown in Fig. 2(b) on polystyrene. The glass thicknesses have been adjusted for matching linear chirp of pump and Stokes. The spectral resolution is limited by the pump pulse duration since the Stokes is longer because of its larger spectral width. Tuning the pump pulse duration from 0.42 to 1.15 ps, the expected<sup>3</sup> excitation resolution  $\Delta$  changes from 42 to  $13\text{ cm}^{-1}$ . The resolution in CARS is about twice

larger due to the readout of the vibration by the pump. The measured spectra confirms this expectation. Increasing the resolution means the CARS intensity is decreasing, showing that the implemented spectral focusing method allows optimizing the trade-off between resolution and signal strength.

As a first proof-of-principle demonstration of CARS and D-CARS micro-spectroscopy, we imaged lipid droplets (mixed glyceryl trioleate and glyceryl trilinolenate) of 1 to  $10\text{ }\mu\text{m}$  diameter in agarose gel. We used  $L_1 = 3\text{ cm}$  and  $L_2 = 0\text{ cm}$  for maximum CARS signal with  $\Delta = 42\text{ cm}^{-1}$ . The IFD at  $t_0 = 0$  (time overlap of pump–Stokes in first pair) is  $3134\text{ cm}^{-1}$ . By varying  $t_0$  from 1.6 to  $-1.6\text{ ps}$ , we tuned the IFD from 2430 to  $3838\text{ cm}^{-1}$ . The power was 34 mW for pump and 8 mW for Stokes at the sample. The D-CARS imaging used  $L_3 = 3\text{ mm}$  yielding  $\Delta_{\text{IFD}} = 130\text{ cm}^{-1}$ . Images of  $I_{\text{sum}}$  and  $I_{\text{dif}}$  are shown in Fig. 3(a) and 3(b). We used  $t_0 = 0.2\text{ ps}$  to have  $\text{IFD}_1 = 3050\text{ cm}^{-1}$  and  $\text{IFD}_2 = 2920\text{ cm}^{-1}$ , near the minimum and maximum CARS signal of the CH stretch band of lipids.  $I_{\text{sum}}$  shows the in-focus droplets, but also shadows from the modulated nonresonant CARS due to excitation beam distortion by the refractive index contrast of the lipid droplets ( $n = 1.49$  compared with  $n = 1.34$  for agar) on the beam path to the focus plane. In the  $I_{\text{dif}}$  images, these shadows are suppressed together with the nonresonant background, and only the lipid droplets in the focus plane are visible.

To demonstrate the advantages of D-CARS as a technique combining label-free chemical contrast with 3-D intrinsic spatial resolution (optical sectioning) and image acquisition speed suitable for living cells, we show in Fig. 3(c) CARS and in Fig. 3(d) D-CARS micro-spectroscopy of living mouse oocytes. Note that the diagnosis of live oocyte quality and fertilization viability in reproductive medicine is still a major issue, where CARS microscopy has the potential to provide a breakthrough owing to its chemical sensitivity compared with currently available label-free techniques such as differential interference contrast. The IFDs in Fig. 3(c) and 3(d) were chosen as for the lipids in Fig. 3(a) and 3(b). Resulting images are shown in Fig. 3(c) and 3(d). Sum-CARS and D-CARS were measured simultaneously, hence show no artifacts due to sample movement. The presence of lipid droplets in the oocyte is clearly visible at the CH vibrational resonance, and the nonresonant background in sum-CARS is suppressed in the D-CARS image.

As a demonstration of correlative fluorescence and CARS microscopy made available by the upgrade of the Zeiss LSM 510 with our module, we shown in Fig. 3(e) adipocytes from 3T3 cell line where lipid droplets were stained with oil-red.

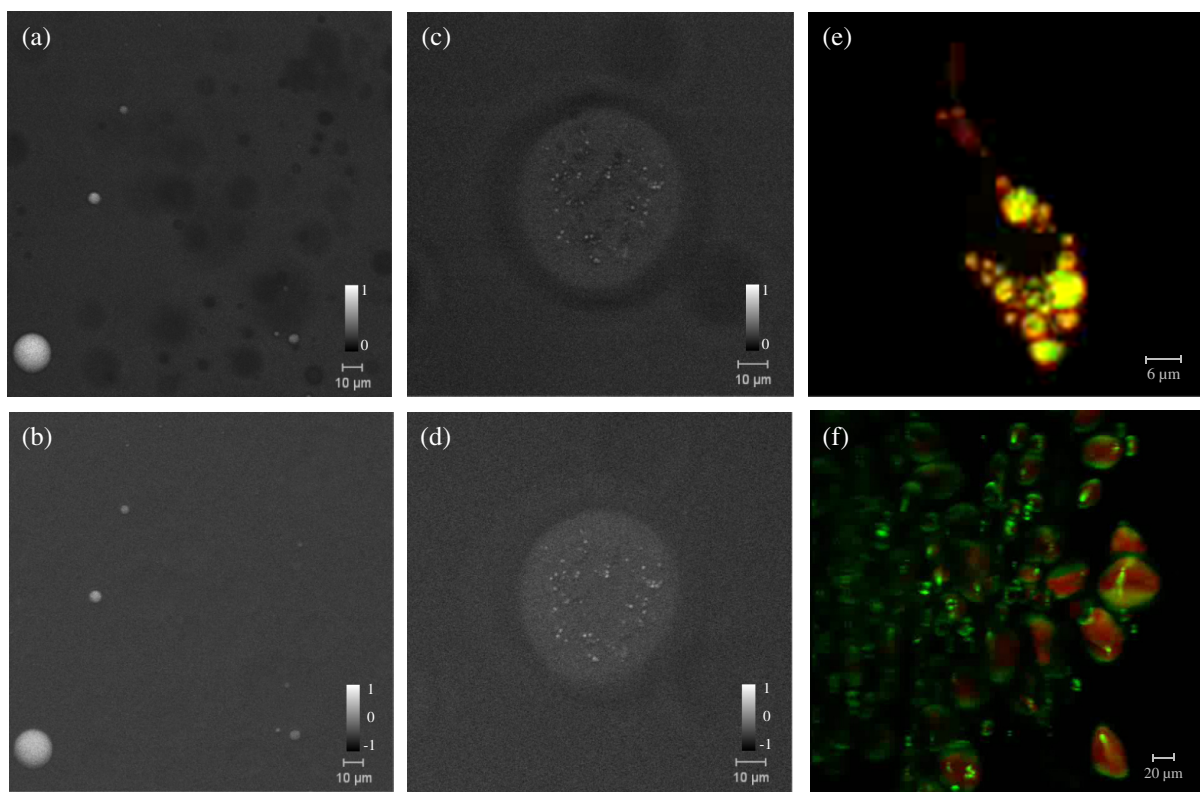


**Fig. 3** Images of lipid droplets in agar of  $196 \times 196 \mu\text{m}^2$  with  $512 \times 512$  pixels acquired at  $7.6 \mu\text{s}/\text{pixel}$ . (a)  $I_{\text{sum}}$ , linear gray scale from 0 (black). (b)  $I_{\text{diff}}$ , linear gray scale symmetric around zero (gray). Images of mouse oocytes (c)  $I_{\text{sum}}$ , linear gray scale from 0 (black). (d)  $I_{\text{diff}}$ , linear gray scale symmetric around zero (gray). The acquisition time was 3.94 s for each image of  $131 \times 131 \mu\text{m}^2$  ( $512 \times 512$  pixels,  $15 \mu\text{s}/\text{pixel}$ ). (e) Adipocytes from 3T3 cell line. Green, differential CARS (D-CARS); red, Oil-red confocal fluorescence. Section  $65 \times 65 \mu\text{m}^2$  of a three-dimensional (3-D) stack (Video 2)  $197 \times 197 \times 20 \mu\text{m}^3$ . (f) D-CARS (red) and SHG (green) of a potato slice in water section of a 3-D stack (Video 3)  $400 \times 400 \times 100 \mu\text{m}^3$  (Video 2, MPEG, 1.4 MB [URL: <http://dx.doi.org/10.1117/1.JBO.18.6.066004.2>]; Video 3, MPEG, 2.2 MB [URL: <http://dx.doi.org/10.1117/1.JBO.18.6.066004.3>]).

Two images were acquired and overlaid. The red contrast is the result of confocal fluorescence acquisition from the microscope original functionality without passing through the D-CARS setup, and the green contrast is the D-CARS image. The D-CARS is adjusted to  $\text{IFD}_1 = 3020 \text{ cm}^{-1}$  and  $\text{IFD}_2 = 2870 \text{ cm}^{-1}$ . As expected, the oil-red staining of lipids gives a similar image to the D-CARS contrast, although some differences are noted. Indeed, it is known that lipid staining is not always representative of the intrinsic lipid content in cells and that fluorescence microscopy is subject to staining artifacts. Food can be imaged well with the system using CARS and SHG, as shown in Fig. 3(f), and the related movie for a potato slice.

#### 4 Conclusions

We have developed and demonstrated a module providing D-CARS contrast for commercial multiphoton microscopes using the available Ti:sapphire oscillator. It allows one to adjust the pulse length and spectral resolution using spectral focusing for an optimal compromise between CARS signal strength and spectral resolution. Hyperspectral CARS images [Fig. 3(f)] are taken by adjusting the pump delay with a frequency step time of about 100 ms, without the complexity of multiplex detection or laser tuning. In the present configuration, Raman frequencies of  $2000$  to  $4000 \text{ cm}^{-1}$  as well as a spectral resolution of  $20$  to  $80 \text{ cm}^{-1}$  is achieved. This range can be extended down to

$1000 \text{ cm}^{-1}$  using different filters, covering part of the characteristic vibrational region enabling higher chemical specificity.

#### Acknowledgments

The authors would like to thank Nick White for technical support with operating the Zeiss LSM510 microscope, Karl Swann for providing the mouse oocytes, Francesco Masia and Adam Glen for providing the oil-red stained adipocytes, and Claudia Di Napoli for providing the lipid droplets in agarose gel. The work was supported by the BBSRC UK research Council under the Follow-on Fund project BB/FOF/297 and the Grant No. BB/H006575/1, by the Cardiff Partnership Fund and by the EPSRC Institutional Grant EP/K503344/1. Paola Borri is a Leadership fellow of the EPSRC UK Research Council (Grant No. EP/I005072/1).

#### References

1. C. L. Evans and X. S. Xie, "Coherent anti-stokes Raman scattering microscopy: chemical imaging for biology and medicine," *Annu. Rev. Anal. Chem.* **1**, 883–909 (2008).
2. H. A. Rinia et al., "Quantitative label-free imaging of lipid composition and packing of individual cellular lipid droplets using multiplex CARS microscopy," *Biophys. J.* **95**(10), 4908–4914 (2008).
3. W. Langbein, I. Rocha-Mendoza, and P. Borri, "Coherent anti-stokes Raman micro-spectroscopy using spectral focusing: theory and experiment," *J. Raman Spectrosc.* **40**(7), 800–808 (2009).

4. T. Hellerer, A. M. Enejder, and A. Zumbusch, "Spectral focusing: high spectral resolution spectroscopy with broad-bandwidth laser pulses," *Appl. Phys. Lett.* **85**(1), 25–27 (2004).
5. K. M. Hilligsoe et al., "Supercontinuum generation in a photonic crystal fiber with two zero dispersion wavelengths," *Opt. Express* **12**(6), 1045–1054 (2004).
6. A. F. Pegoraro et al., "Optimally chirped multimodal CARS microscopy based on a single Ti:sapphire oscillator," *Opt. Express* **17**(4), 2984–2996 (2009).
7. I. Rocha-Mendoza et al., "Differential coherent anti-Stokes Raman scattering microscopy with linearly-chirped femtosecond laser pulses," *Opt. Lett.* **34**(15), 2258–2260 (2009).
8. I. Rocha-Mendoza, P. Borri, and W. Langbein, "Quadruplex CARS micro-spectroscopy," *J. Raman Spectrosc.* **44**(2), 255–261 (2013).